Coulomb blockade effects in Ag/Si(111): The role of the wetting layer

Jędrzej Schmeidel, Herbert Pfnür, and Christoph Tegenkamp
Institut für Festkörperphysik, Leibniz-Universität Hannover, 30167 Hannover, Germany
(Received 11 June 2009; revised manuscript received 7 August 2009; published 4 September 2009)

Single and double barrier structures have been realized with Ag nanostructures grown on Si(111) in combination with scanning tunneling microscopy. The series connection of a Schottky (SB) and tunneling barrier mimics a double barrier structure showing Coulomb blockade oscillations as revealed by scanning tunneling spectroscopy (STS). Although the SB remains in presence of a Ag$\sqrt{3}\times\sqrt{3}$ reconstruction, the dI/dV characteristic turns into a single barrier structure. The Ag reconstruction provides a sufficiently high electron mobility capturing intrinsic defects which shortens the resistance of the SB. These results show that vertical transport properties, as measured with STS, are not only controlled by the structure and the bonding on the atomic scale, but depend strongly on the lateral properties of the interface as well.

DOI: 10.1103/PhysRevB.80.115304 PACS number(s): 07.79.Cz, 63.22.Kn, 73.23.Hk, 73.30.+y

I. INTRODUCTION

Thin metallic adlayers on semiconductor surfaces have attracted much research interest recently as they are model systems for highly correlated $2d$ and $1d$ electron gases.[1–4] At low temperatures the semiconducting host is insulating, i.e., these systems can be used to correlate morphology with electronic band structure, transport, and even superconductivity at the atomic scale.[5–8]

Since for semiconductor heterostructures with ultralow electron concentrations Fermi wavelengths can be of the order of 100 nm, size quantization or Coulomb blockade (CB) effects are comparably easy to observe in these systems at low temperature. Consequently, the detailed structure of interfaces and defects *on the atomic scale* are only of minor relevance and, thus, (Ohmic) contacts for transport studies are well defined on this length scale. For metallic systems, on the contrary, defects are extremely crucial and, therefore, lateral transport measurements are extremely demanding. For instance, for the surface conductivity values differing by three orders of magnitude are reported in literature for nominally the same system.[9–12]

Generally, metallic adlayers or ultrasmall metallic islands on semiconductor surfaces are prototype systems for studies of contact properties since they allow detailed insight into the contact formation. Since the fabrication of Ohmic contacts, in particular on the atomic scale, always bears the problem of irreversible changes while forming the contact, the tunneling contact is conceptually more appropriate to elucidate the properties of nanosized contacts including proximity and size effects. Only very few attempts have been reported, in which the interrelation between vertical and lateral conductivity measurements was explicitly addressed.[11] However, as we will show, these are closely coupled, i.e., the properties seen in scanning tunneling spectroscopy (STS) are related to surface conductivity. This problem becomes particularly relevant when different types of contacts are formed, e.g., in combination with single adsorbed molecules.

In order to study systematically the influence of surface structures on mesoscopic properties, some versatility in the system is required. The Ag/Si(111) system is particularly suitable because different morphologies with characteristic band structures can be realized[13] mimicking mesoscopic systems: concepts of wetting layers, Schottky barrier (SB), epitaxial growth can be used to tune systematically mesoscopic parameters, e.g., capacitance and resistance. In combination with a scanning tunneling microscope (STM), double junction barriers can be realized as schematically shown in Fig. 1: the SB at the interface (inner potential V_{SB}) separates adlayers and nanostructures electronically from the underlying substrate. It can be tuned by the metal/semiconductor material combination and the dopant concentration. The tunneling resistance $R_{t,1}$ is adjustable by the STM and in conjunction with $R_{t,2}=(R_{SB}\|R_{leak})$ should be large compared to $h/e^2=25.8$ kΩ, in order to have defined tunneling barriers in the vertical direction, i.e., normal to the surface or interface. Here R_{leak} denotes a parasitic pathway for the tunneling current and its value depends critically on the interface, e.g., sheet resistance, and defect concentration. The capacitance C of the tunneling junction, which determines the charging energy for a single electron e^2/C, is given for this setup by the tunneling distance and the Debye length λ_D, respectively, and an *effective area*, which is tunable by the lateral extension of the surface structure. If the charging energy is large compared to the thermal energy in the system ($e^2/C \gg k_bT$), single electron tunneling occurs along this double barrier structure.

In this paper, we try to elucidate the role of surface layers and of their structural as well as of their electronic properties

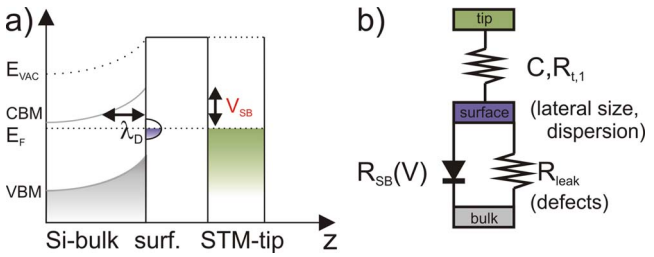

FIG. 1. (Color online) (a) Energy diagram of the metal/semiconductor heterojunction at zero bias including the Schottky barrier and the tunneling barrier between STM tip and metal island. (b) Equivalent circuit of (a) with the most relevant electrical parameters. For details see text.

on the tunneling behavior between a metal tip and a (low doped) Si bulk material. We will present STS results performed on different Ag/Si(111) interface structures. We start with the spectroscopy of the perfect surface phases as reference. Thereafter, the realization of single and double tunneling barrier structures with Ag clusters is presented. Finally, this finding is discussed in terms of the band structure and the in-plane conductivity.

As we will show, these are realizations of mesoscopic systems, which allow to tune selectively the properties of the quantum dot (QD) structure. Thus we obtain the possibility to study the influence of size effects, of the electronic band structure as well as of the injection process of the electrons, which is difficult to control in systems realized by semiconductor heterostructures.

II. EXPERIMENTAL SETUP

The experiments were performed in an ultrahigh vacuum system consisting of two connected chambers. Both operate at a base pressure of 1×10^{-9} Pa. The preparation chamber is equipped with low-energy electron diffraction (LEED) and x-ray photoelectron spectroscopy (XPS) to control the overall quality of the morphology and the chemistry of the surface before transferring the sample into the variable temperature STM (RHK) located in the main chamber. Clean Si(111) (n-doped, $N_D=10^{17}$ cm^{-3}, 0.01 Ωcm) surfaces were obtained after several heating cycles up to 1400 K by direct current heating. Ag was evaporated out of a glossy carbon crucible, which was heated by electron bombardment (1 kV, 20 mA). A semimetallic Ag$\sqrt{3}\times\sqrt{3}$ wetting layer was obtained by annealing the sample to 800 K for several minutes. Nanosized Ag islands were generated by evaporation of Ag at low temperatures followed by annealing to 300 K. The microscopy and spectroscopy was performed at 80 K (LN_2). The presented $I(V)$ curves were obtained by averaging at least ten individual $I(V)$ curves, differentiation was done numerically. The morphology was checked before and after local spectroscopy in order to rule out thermal drift and/or tip induced changes to the surface. Temperatures above 670 K were measured pyrometrically, while the low-temperature regime was controlled by a Ni/NiCr thermocouple mounted to the sample holder.

III. RESULTS AND DISCUSSION

A. Si(111) and Ag$\sqrt{3}\times\sqrt{3}$ surface structures

Starting with the clean Si(111)-(7×7) reconstructed surface [shown in Fig. 2(a)], local spectroscopy reveals nicely the characteristic gap as shown in Fig. 2(c). Within the gap the occupied $S1$ and $S2$ states at negative bias voltages are clearly visible, which originate from different re-bonding configurations of adatoms and rest atoms.[14] In particular, the unoccupied state around +0.7 V is strongly pronounced, in good agreement with other experiments.[15] Due to the difference of the chemical potential at the surface and of the n-type Si bulk material, band bending occurs. The Schottky barrier [V_{SB}, cf. with Fig. 1(a)] is around 0.5 eV, as can be judged from the symmetry of the band structure with respect

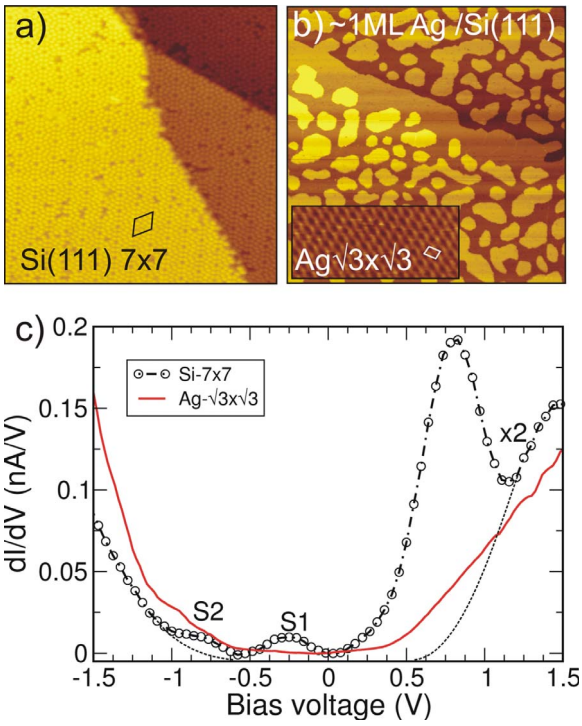

FIG. 2. (Color online) (a) Topography of the Si(111) 7×7 reconstruction (size 30×30 nm^2) and (b) of the Ag$\sqrt{3}\times\sqrt{3}$ structure after adsorption of one monolayer of Ag and annealing to 820 K (size 300×300 nm^2). Inset: Ag islands (size 7.4×3.2 nm^2). Tunneling parameters were +2 V, 0.5 nA (inset: +1 V, 0.4 nA). (c) STS spectra taken on both surfaces. The dashed lines are guides to the eye in order to illustrate the bandgap without surface states.

to zero bias. The residual tunneling current at +100 mV sample bias is on the order of 10 pA; i.e., the resistance of the SB limited by residual defects is ≈10 GΩ. As we will demonstrate below, the SB and the tunneling barrier (TB) at the vacuum side in series represent either single or double tunneling barriers, which are tunable by modifying the interface properties. In order to have quite symmetric resistances in the double barrier structure, the set point (SP) for STS was appropriately chosen, e.g., 0.2 nA and 2 V.

Since the Debye length λ_D in our low-doped samples is on the order of 100 nm, electron transport (of the majority, i.e., of electrons) along the surface normal is controlled by thermal excitation rather than by electron tunneling.[16] Therefore, normal to the surface only transport via hopping along defect sites can depopulate surface states giving rise to a parasitic pathway denoted by R_{leak} in Fig. 1(b). Typically, this is the classical pathway for electrons since the direct connection to Ohmic contacts is not guaranteed. From the dopant concentration a two-dimensional defect concentration of 10^{12} cm^{-2} (one defect state per 30^2 lattice constants) is estimated. Transport to these channels conducting normal to the surface by hopping transport, however, can be effective only if the surface states provide a sufficiently high electron mobility within the surface plane. Otherwise, local charging occurs. Therefore, for any (semi)metallic structures on semiconducting templates, where the electronic structures are decoupled from each other, the lateral transport properties, i.e.,

the $2d$ dispersing bands are crucial for local spectroscopy as well.

A well-characterized homogeneous interface structure is the Ag$\sqrt{3}\times\sqrt{3}$ reconstruction on Si(111). It is formed when 1 monolayer (ML) Ag is adsorbed followed by annealing to 800 K for several minutes [cf. with inset of Fig. 2(b)]. Upon the Ag-Si bond formation, the exchange of Si atoms leads to the formation of a distinct two-level roughness of a formerly atomically smooth Si(111) terrace as Fig. 2 shows. The local structure is described by the honeycomb-chained triangle (HCT) and inequivalent triangle (IET) model at RT and low temperatures, respectively.[13,17,18] The corresponding dI/dV curve is shown in Fig. 2. The surface states of the clean Si surface are not visible any longer. Although the overall conductance is slightly increased with respect to the Si(111) sample, the Ag$\sqrt{3}\times\sqrt{3}$ surface provides obviously only a low density of states around the Fermi level in this well ordered layer. For tunneling is appears transparent for reasons explained in detail below.[19,20]

In order to understand our STS results the electronic properties of the Ag$\sqrt{3}\times\sqrt{3}$ layer are important. If exactly 1 ML is adsorbed, the SB is even enlarged by 0.3 eV, as seen by angle resolved photoemission (ARPES) and as demonstrated by the asymmetry of the dI/dV curve with respect to zero bias. As revealed by ARPES further, the perfect wetting layer is only half-metallic,[21] i.e., there is no gap, but the occupied states barely touch the Fermi surface. A two-dimensional electron gas is only formed by electrons originating from excess Ag coverage that fill previously unoccupied electronic states. In fact, this reduces slightly the SB, but V_{SB} still remains ≥ 0.5 eV, i.e., the R_{SB} contribution of $R_{t,2}$ between the surface and the bulk is either increased or remains the same as for the uncovered Si surface. However, compared to the clean Si(111) surface, the electronic structure within the plane has changed giving rise to different lateral mobilities and, therefore, to an enlarged R_{leak} contribution. This alone cannot explain our observations.

However, the spectroscopy done with STM, is in fact a transport measurement. Thus, peaks in dI/dV curves originate from resonances induced by electronic states, e.g., surfaces states, in between the sample-tip configuration. Therefore, apart from the density of states two further aspects for the involved electronic states are of importance: First, the dispersion determines whether a resonant injection is possible. Since the tip is a point source, the momentum distribution is *a priori* broad and depends in detail on the tunneling distance and on the lateral extension of the structure. Consequently, resonant coupling is more effective for localized states or for band structures with small dispersion. Second, the lifetime of electrons in the electronic states has to be sufficiently large in order to enhance the tunneling probability. Otherwise, the states of the nanostructure appear transparent in local spectroscopy, although the structure itself maybe highly metallic. This is how the lateral size of the structure and the dispersion come into play, as these quantities control the R_{leak} contribution in the proposed model.

The appearance of resonances of the surface states in the dI/dV signal of the clean Si(111) surface and their absence in the Ag$\sqrt{3}\times\sqrt{3}$ structure can be explained by these considerations: In contrast to Si(111), the surface bands of the Ag$\sqrt{3}\times\sqrt{3}$ are strongly dispersing as seen by ARPES.[21,22] The delocalized character is manifested in a high electron mobility giving rise to a low sheet resistance. For the same reason Shockley surface states on noble metal surfaces, are barely resolvable either.

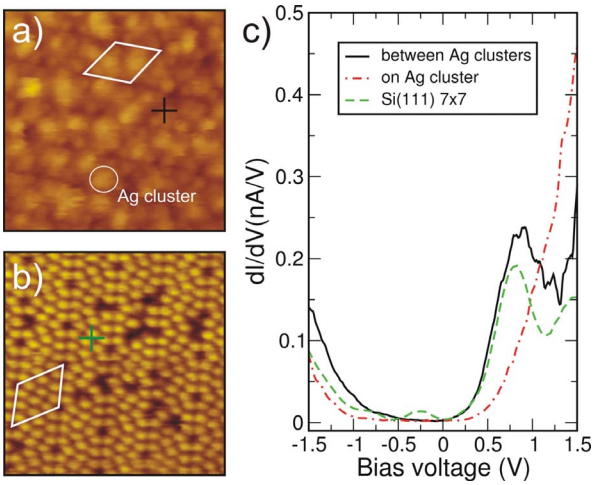

FIG. 3. (Color online) (a) STM graph after adsorption of 0.2 ML Ag at 80 K. The comparison with the corner hole structure of the clean Si(111) surface (b) shows that the Ag clusters are aligned along the (7×7) reconstruction. Both images are 10×10 nm^2 taken at (a) −2 V. 0.05 and (b) +2 V, 0.2 nA. The unit cell vectors of the (7×7) structure are shown as well. (c) dI/dV spectra taken on [dashed-dotted (red) line] and in between [solid (black) line] the clusters at the position marked by a circle and cross in (a), respectively. The robust unoccupied Si-surface state is still visible in between the Ag clusters. For comparison, the spectrum of the clean surface is shown as well [dashed (green) line].

The conclusion drawn from these atomic systems shall be verified in the following by performing STS on Ag nanostructures grown on Si(111) varying both the size and the environment (wetting layer). As we will show, the wetting layer is of importance as it can be used to trigger different mesoscopic transport regimes.

B. Isolated Ag clusters on Si(111): CB oscillations

Adsorption of Ag at low temperatures in the submonolayer regime without subsequent high temperature annealing steps does not form a wetting layer. This is demonstrated in Fig. 3. Here we evaporated 0.2 ML Ag on a Si(111) surface at 80 K. Annealing to only 100 K leads to some ordering, as can be seen in Fig. 3(a). Obviously, the Ag atoms occupy specific sites within the (7×7) surface cell, as the corner hole structure is still visible. At the positions marked by the circle and the cross in Fig. 3(a) dI/dV curves have been taken. As can be seen from Fig. 3(c) in between the protrusions the characteristic unoccupied surface state of the (7×7) reconstruction is still seen (cf. with Fig. 2), i.e., an intact Si surface remains between the Ag clusters, while for STS on top of the Ag clusters this state has disappeared. Further spectroscopic details are discussed in the context of larger Ag islands presented in the following.

Larger, but still nonpercolated Ag islands are formed, if Ag is adsorbed at low temperatures and annealed to 300 K

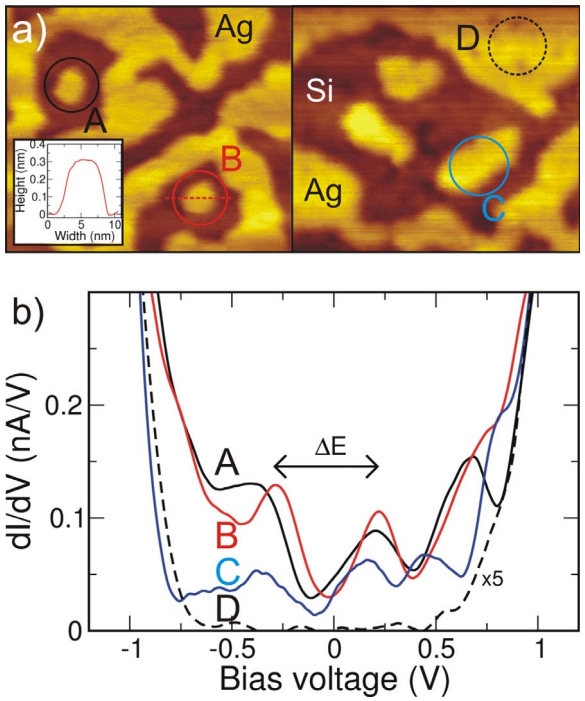

FIG. 4. (Color online) (a) Different Ag islands (labeled A–D) of monatomic height on Si(111) after adsorption of 0.6 ML Ag at 80 K and annealing to 300 K. Image sizes 43×50 nm^2 (+2 V,0.5 nA). The inset shows a line scan through island B. (b) dI/dV measurements (SP:+1.5 V, 0.5 nA, except island C:+2 V, 0.5 nA) taken on four different Ag islands. Only for nonpercolated Ag islands (A–C) pronounced CB oscillations are seen in the Si gap window.

[see Fig. 4(a), initial coverage 0.6 ML]. Compared to the dI/dV curves seen on the clean surfaces, the spectroscopy on these islands, labeled A–C in Fig. 4(b), reveals a completely different behavior. Equidistant peaks appear and are easily resolvable in the bias range from −1 to +1 V. The appearance of such resonances is the signature of an *effective* double barrier structure along the tunneling pathway.

These oscillations must be due to the CB effect, where electrons are tunneling one by one through the Ag QD. Since the film thickness of these islands presented above is only one monolayer [cf. with line scan inset in Fig. 4(a)], resonances induced by, e.g., quantum well states (QWSs), which have been observed by STS for similar metal/semiconductor systems,[23,24] can be ruled out here. The energetic separation of QWS can be roughly estimated by $\Delta=\pi\hbar v_F/D$, where $\hbar$, v_F, and D denote Planck's constant, the Fermi velocity and the film thickness, respectively. Hence, for epitaxially grown Ag films on Si(111) a height of at least ten layers is needed to observe a splitting of around 1 eV for QWS [$v_F=1.4\times10^8$ cm/s, (111) texture], which is clearly outside the coverage range investigated here.

From the voltage separation of the oscillations the capacitances can easily be determined. The splitting for the three Ag islands, A–C, presented in Fig. 4(a) varies between 0.4 and 0.6 eV; i.e., the capacitances of the tunneling junction are between 0.26 and 0.4 aF. The associated capacitances are small enough so that CB oscillations can be seen already at $T=80$ K. Systematic studies of the Coulomb suppression in single tunneling junction assemblies have shown that the capacitance of the junction is inversely proportional to the sample-tip distance d,[25] i.e., the junction geometry can be described as a simple parallel capacitor with a capacitance $C=\epsilon\epsilon_O A/d$, where A is the effective capacitive area. With a typical sample-tip distance around 1 nm, the effective area is of the order of 30–50 nm^2 ($\epsilon=1$ for vacuum), which is in good agreement with the Ag island size. Compared to former studies,[25,26] the epitaxial systems in our case are prepared and investigated *in situ* so that STM can be used to characterize reliably the structure as well.

With these estimates of the capacitances of islands A–C, it is clear that the islands shown in Fig. 3 with an average diameter of only 1 nm must have a capacitance below 0.01 aF. With this low capacitance the peak separation of CB is outside the window of ±1 V, in agreement with our observation. Therefore, CB is the dominating effect for all these islands without wetting layer.

Apart from the size-dependent peak separation, another size effect is visible in Fig. 4: While the oscillations get smaller with increasing island size, also the average tunneling current goes down. For the dI/dV spectrum taken on-top of the extended island D, no CB oscillations are seen at all [dashed line in Fig. 4(c)]. In terms of conductivity, this behavior is at first sight unexpected, but in line with the conclusions drawn from the STS spectra taken on surface states.

This gradual disappearance of resonances must be caused again by a reduction of electron life time in a particular energetic state, i.e., by a similar effect as discussed above for the Ag$\sqrt{3}\times\sqrt{3}$ layer. Formation of a two-dimensional band structure within the islands allows delocalization and energetic redistribution of the incoming electrons, which gets more effective with increasing size of the islands. In addition, as the Ag islands grow in size, a sufficient number of defects at the interface is captured, thus reducing the lifetime further so that the island itself is transparent in spectroscopy.

C. Ag multilayers: the role of the wetting layer

The last subsection has shown that nonpercolated Ag islands grown on Si(111) are a prototype structure for a double barrier junction showing CB oscillations. Surprisingly, these signatures survive even if up to 3 ML Ag are deposited at low temperatures so that no Ag$\sqrt{3}\times\sqrt{3}$ wetting layer exists. In this particular case annealing to 300 K forms a granular film, as shown in Fig. 5(a). Clearly visible is the oscillatory behavior in the vertical conductivity [Fig. 5(b)]. The slight asymmetry in the dI/dV curve in Fig. 5(b) may be caused by the local inhomogeneity induced by the adjacent clusters. As the grain size is comparable with the islands A–C discussed in context with Fig. 4, the oscillation period in conductivity is similar. The main difference to the islands investigated in Fig. 4 is that the overall characteristic of the film conductance is metallic and the Si band gap is no longer visible in the $I(V)$ curve. This means that the film was obviously percolated on a macroscopic scale and had a direct connection with the macroscopic bias contact, i.e., the resistance of the Ag film itself is probed by STS. These findings are in agree-

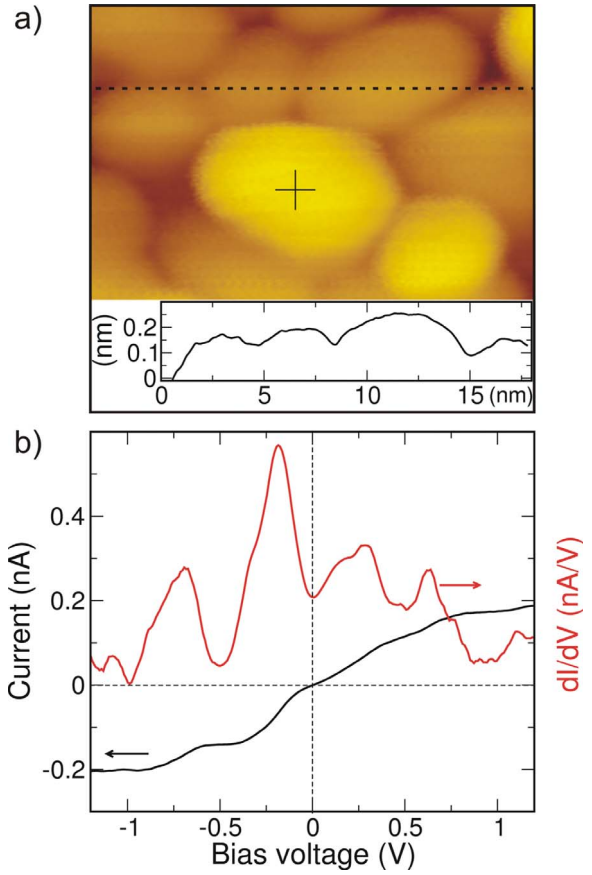

FIG. 5. (Color online) (a) 3 ML Ag film annealed to 300 K forming a granular film structure on Si(111). Scan size 18 $\times 13.5$ nm^2 (SP: −1.5 V, 0.25 nA). The line scan taken along the dashed line shows the percolation of adjacent Ag clusters. (b) $I(V)$ and dI/dV curves taken at the cluster in (a) at the cross-marked position showing CB oscillations.

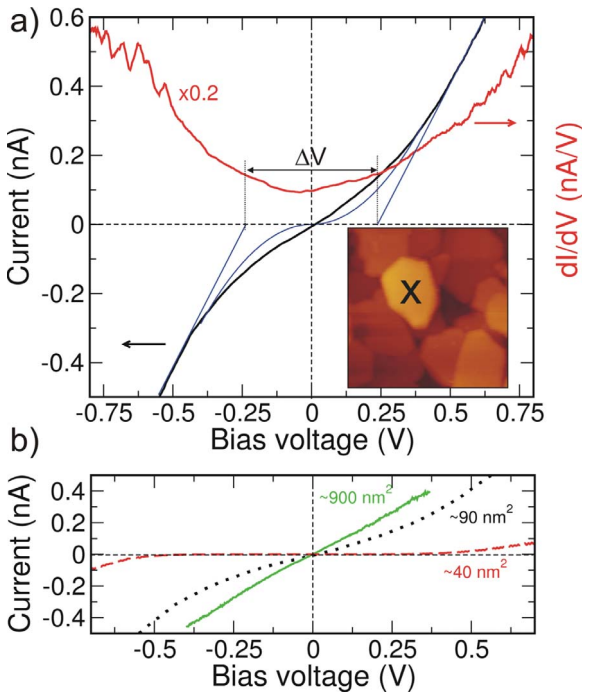

FIG. 6. (Color online) (a) $I(V)$ (black) and dI/dV curves (red) taken above a crystallographically well ordered Ag islands grown on an Ag wetting layer (inset: 40×40 nm^2). The set point for the $I(V)$ curve was +0.5 V, 0.3 nA. The voltage gap ΔV in between the intersections is intimately related to the capacitance C of the tunnel junction ($\Delta V=e/C$). The blue lines represent asymptotes at high biases and a quadratic fit in the low bias regime using $R_t=1$ GΩ and C=0.4 aF. For further details see text. (b) IV curves taken above Ag islands of different sizes.

ment with previous investigations of Ag film conductance on a macroscopic scale.[27] Here a nonmetallic conductivity for a similar thin Ag-film structure has been reported using a macroscopic four-point probe technique in a Van-der-Pauw geometry. Consistent with our STS results, the authors identified the CB limited tunneling between the grains as a likely mechanism for the transport in this system.[27]

The transport characteristics of a double junction barrier change to single barrier properties, if Ag islands are evaporated onto an Ag$\sqrt{3}\times\sqrt{3}$ reconstruction. The inset of Fig. 6(a) shows such Ag islands. The shape of the islands is close to hexagonal, i.e., the adislands are crystalline and well oriented in presence of a wetting layer. The corresponding dI/dV curve taken at the island marked by a cross is shown in Fig. 6(a) as well. They do not contain any oscillations, although the epitaxial Ag islands have a size comparable to those, where we found CB oscillations without the wetting layer. The current varies nonlinearly with voltage in the low bias regime, while it varies linearly at high bias voltages. This type of $I(V)$ curves is characteristic of single tunneling junction barriers, where only a suppression of charge transfer is seen and oscillations are averaged out due to stray capacitances within the experimental setup. If the current is suppressed by CB at low voltages, the displacement of the asymptotes $\Delta V=0.4$ V is related to the capacitance via $C=e/\Delta V=0.4$ aF, which is again of the same order as that obtained for the islands shown above. In order to demonstrate the size dependence, Fig. 6(b) shows three IV curves taken above Ag islands of different sizes. In qualitative agreement with the simple model for the capacitance of the tunneling junction, the pseudogaps in between the extrapolated linear regimes become smaller as the islands become larger. A quantitative treatment of this size dependence would give more insight into the influence of the shape and the neighborhood of the islands, but this was beyond the scope of this work.

The values of the capacitance and of the tunneling resistance can be independently determined since the entire $I(V)$ curve depends only on R_t and C via $I=(2C/\pi R_t e)\ V^2$ (Ref. 28) in the low voltage regime (assuming zero temperature), as exemplarily shown for the IV curve of Fig. 6(a). This parameter-free curve [thin drawn (blue) curve in Fig. 6(a)] is in reasonable agreement with the experiment. The deviation points toward parasitic leakage currents, which add a linear voltage dependence in the low bias regime. A similar behavior has been found, for instance, for granular stainless steel films.[26]

Besides the suppression due to CB of the current in the low bias regime, the average conductivity is significantly higher compared to the bare $\sqrt{3}$ phase presented in Fig. 2.

This can be understood because additionally adsorbed Ag, nucleated at step sites, forms *vias* between adjacent Ag$\sqrt{3}\times\sqrt{3}$ reconstructed terraces and, thus, lowers the in-plane resistivity.

Apart from this leakage current effect, it should be pointed out that, irrespective of the presence of the wetting layer, the SB at the surface remains nearly unchanged, as concluded from photoemission experiments.[21] Therefore, the lateral properties of the Ag$\sqrt{3}\times\sqrt{3}$ reconstruction themselves must be responsible for the transition from the double to an effective single tunneling barrier. According to the equivalent circuit diagram of the heterostructure (cf. with Fig. 1), R_{leak} must be significantly decreased.

R_{leak} can be decreased either by increasing the defect concentration within the whole depletion layer of the Si interface. It is very unlikely that the generation of the Ag$\sqrt{3}\times\sqrt{3}$ wetting layer, which is well ordered, is the source of such an effect. Starting from the defect concentration for the clean Si(111) surface mentioned above, nearly every lattice site would have to be coupled via defect states to the bulk material in order to decrease R_{leak} by three orders of magnitude. In fact the Ag$\sqrt{3}\times\sqrt{3}$ structure shows many domain boundaries [cf. with Fig. 2(b)], but their concentration is still insufficient.[13] Also bulk silicide formation with Ag is not possible under our conditions. Alternatively, the mobility of the electrons within the wetting layer must be orders of magnitude higher than on the Si surface without wetting layer, and coupling between the Ag islands and the wetting layer must be strong. The latter has to be expected for Ag islands on an Ag wetting layer. Thus resonances within an individual island disappear. High electron mobility and the absence of resonances in STS due to a significantly dispersing band structure within the wetting layer has already been concluded from the results of the perfect Ag$\sqrt{3}\times\sqrt{3}$ structure. Accordingly, the diffusion of the electrons in the plane is increased, i.e., without changing significantly the initial defect concentration, the spread of the electrons is responsible for a sufficiently low R_{leak} resistance, which overcompensates the (local) Schottky barrier resistance R_{SB}. This is qualitatively in agreement with the conductivity observed in lateral transport measurements using a four point-probe technique on the micrometer scale.[29] Compared to the (7×7) reconstruction, the resistance is lowered by three orders of magnitude for the Ag$\sqrt{3}\times\sqrt{3}$ at low temperatures (100 K).[29]

IV. SUMMARY AND OUTLOOK

In summary, we explored the occurrence of effective single and double barriers in tunneling microscopy and spectroscopy for the Ag/Si(111) system in the monolayer regime by varying the preparation conditions. Although STM and STS are local probes, the results obtained with these methods can well be correlated with mesoscopic transport phenomena and provide a more detailed insight into the underlying mechanisms.

It is obvious that the formation of double barriers and the observation of corresponding resonances requires localization of electrons at the surface, i.e., between the SB formed at the Si surface and the tunneling barrier to the tip. This localization is already possible to a measurable extent in the weakly dispersing surface states of the clean Si(111) (7×7) surface, whereas the tunneling electrons get delocalized in the Ag$\sqrt{3}\times\sqrt{3}$ layer with its strong two-dimensional dispersion, and no resonances can be detected, making the Ag$\sqrt{3}\times\sqrt{3}$ layer "transparent" for the tunneling electrons. Two-dimensional localization is also seen in lateral dc conductance measured on mesoscopic or even macroscopic scales, and corroborates the trends seen in STS for our system. Efficient localization on the time scales relevant in tunneling experiments and formation of double barriers was found in all situations where Ag islands were grown directly on the Si(111) surface, i.e., without the $\sqrt{3}$ phase underneath. Corresponding CB oscillations have been found even for granular multilayer Ag films. Similar Ag island structures grown on Ag$\sqrt{3}\times\sqrt{3}$, however, show only a single barrier characteristic.

Our examples show nicely that vertical transport properties, as measured with local tunneling spectroscopy, are not only governed by structure and bonding on the atomic scale, but for a metal/semiconductor interface depend strongly also on the lateral two-dimensional properties of the interface. These properties are related to lateral transport properties and should be considered if STS is performed on surfaces with tunable band gaps.

ACKNOWLEDGMENTS

Financial support by the Deutsche Forschungsgemeinschaft is gratefully acknowledged.

[1] T. Kanagawa, R. Hobara, I. Matsuda, T. Tanikawa, A. Natori, and S. Hasegawa, Phys. Rev. Lett. **91**, 036805 (2003).
[2] J. N. Crain, A. Kirakosian, K. N. Altmann, C. Bromberger, S. C. Erwin, J. L. McChesney, J. L. Lin, and F. J. Himpsel, Phys. Rev. Lett. **90**, 176805 (2003).
[3] H. W. Yeom, S. Takeda, E. Rotenberg, I. Matsuda, K. Horikoshi, J. Schaefer, C. M. Lee, S. D. Kevan, T. Ohta, T. Nagao, and S. Hasegawa, Phys. Rev. Lett. **82**, 4898 (1999).
[4] J. R. Ahn, P. G. Kang, K. D. Ryang, and H. W. Yeom, Phys. Rev. Lett. **95**, 196402 (2005).
[5] Ph. Hofmann and J. W. Wells, J. Phys.: Condens. Matter **21**, 013003 (2009).
[6] T. Tanikawa, I. Matsuda, T. Kanagawa, and S. Hasegawa, Phys. Rev. Lett. **93**, 016801 (2004).
[7] C. Tegenkamp, Z. Kallassy, H. Pfnür, H.-L. Günter, V. Zielasek, and M. Henzler, Phys. Rev. Lett. **95**, 176804 (2005).
[8] C. Brun, I-Po Hong, F. Patthey, I. Yu. Sklyadneva, R. Heid, P. M. Echenique, K. P. Bohnen, E. V. Chulkov, and W.-D. Schneider, Phys. Rev. Lett. **102**, 207002 (2009).
[9] K. Yoo and H. H. Weitering, Phys. Rev. B **65**, 115424 (2002).

[10] J. W. Wells, J. F. Kallehauge, T. M. Hansen, and Ph. Hofmann, Phys. Rev. Lett. **97**, 206803 (2006).
[11] S. Heike, S. Watanabe, Y. Wada, and T. Hashizume, Phys. Rev. Lett. **81**, 890 (1998).
[12] T. Tanikawa, K. Yoo, I. Matsuda, S. Hasegawa, and Y. Hasegawa, Phys. Rev. B **68**, 113303 (2003).
[13] S. Hasegawa, N. Sato, I. Shiraki, C. L. Petersen, P. Bøggild, T. M. Hansen, T. Nagao, and F. Grey, Jpn. J. Appl. Phys. **39**, 3815 (2000).
[14] J. E. Northrup, Phys. Rev. Lett. **57**, 154 (1986).
[15] R. J. Hamers, R. M. Tromp, and J. E. Demuth, Phys. Rev. Lett. **56**, 1972 (1986).
[16] S. M. Sze, *Physics of Semiconductor Devices*, 2nd ed. (Wiley Interscience, New York, 1998).
[17] I. Matsuda, H. Morikawa, C. Liu, S. Ohuchi, S. Hasegawa, T. Okuda, T. Kinoshita, C. Ottaviani, A. Cricenti, M. D'angelo, P. Soukiassian, and G. Le Lay, Phys. Rev. B **68**, 085407 (2003).
[18] M. Katayama, R. S. Williams, M. Kato, E. Nomura, and M. Aono, Phys. Rev. Lett. **66**, 2762 (1991).
[19] V. A. Gasparov and M. Riehl-Chudoba, Surf. Sci. **601**, 5403 (2007).
[20] S. Tosch and H. Neddermeyer, Phys. Rev. Lett. **61**, 349 (1988).
[21] J. N. Crain, M. C. Gallagher, J. L. McChesney, M. Bissen, and F. J. Himpsel, Phys. Rev. B **72**, 045312 (2005).
[22] R. I. G. Uhrberg, G. V. Hansson, J. M. Nicholls, P. E. S. Persson, and S. A. Flodström, Phys. Rev. B **31**, 3805 (1985).
[23] Y. Qi, W. Yang, X. Ma, S. Ji, Y. Fu, Y. Zhang, J.-F. Jia, and Q.-K. Xue, J. Phys.: Condens. Matter **19**, 136005 (2007).
[24] I. B. Altfeder, K. A. Matveev, and D. M. Chen, Phys. Rev. Lett. **78**, 2815 (1997).
[25] P. J. M. van Bentum, L. E. C. van de Leemput, R. T. M. Smokers, and H. van Kempen, Phys. Scr. **T25**, 122 (1989).
[26] P. J. M. van Bentum, R. T. M. Smokers, and H. van Kempen, Phys. Rev. Lett. **60**, 2543 (1988).
[27] M. Henzler, T. Lüer, and A. Burdach, Phys. Rev. B **58**, 10046 (1998).
[28] D. V. Averin and K. K. Likharev, J. Low Temp. Phys. **62**, 345 (1986).
[29] I. Matsuda, C. Liu, T. Hirahara, M. Ueno, T. Tanikawa, T. Kanagawa, R. Hobara, S. Yamazaki, S. Hasegawa, and K. Kobayashi, Phys. Rev. Lett. **99**, 146805 (2007).